

We are IntechOpen, the world's leading publisher of Open Access books Built by scientists, for scientists

6,900

Open access books available

186,000

International authors and editors

200M

Downloads

Our authors are among the

154

Countries delivered to

TOP 1%

most cited scientists

12.2%

Contributors from top 500 universities



WEB OF SCIENCE™

Selection of our books indexed in the Book Citation Index
in Web of Science™ Core Collection (BKCI)

Interested in publishing with us?
Contact book.department@intechopen.com

Numbers displayed above are based on latest data collected.
For more information visit www.intechopen.com



Chapter

Nonthermal Crystalline Forming of Ceramic Nanoparticles by Non-Equilibrium Excitation Reaction Field of Electron

Norihiro Shimoi

Abstract

In this work, we have discovered a method of forming ZnO thin films with high mobility, high carrier density and low resistivity on plastic (PET) films using non-equilibrium reaction fields, even when the films are deposited without heating, and we have also found a thin film formation technique using a wet process that is different from conventional deposition techniques. The field emission electron-beam irradiation treatment energetically activates the surface of ZnO particles and decomposes each ZnO particles. The energy transfer between zinc ions and ZnO surface and the oxygen present in the atmosphere around the ZnO particles induce the oxidation of zinc. In addition, the ZnO thin films obtained in this study successfully possess high functional thin films with high electrical properties, including high hole mobility of $208.6 \text{ cm}^2/\text{Vs}$, despite being on PET film substrates. These results contribute to the discovery of a mechanism to create highly functional oxide thin films using a simple two-dimensional process without any heat treatment on the substrate or during film deposition. In addition, we have elucidated the interfacial phenomena and crosslinking mechanisms that occur during the bonding of metal oxide particles, and understood the interfacial physical properties and their effects on the electronic structure. and surface/interface control, and control of higher-order functional properties in metal/ceramics/semiconductor composites, and contribute to the provision of next-generation nanodevice components in a broad sense.

Keywords: non-equilibrium reaction excitation field, field emission, zinc oxide, nanoparticle, conductive ceramic film

1. Introduction

As the Internet of Things (IoT) continues to grow, networks are being built in which various devices share information with each other. At present, data from various devices is scattered and siloed, but it is predicted that in the latter half of the 2020s, hundreds of billions of devices will be connected to the Internet. In the second half of the 2020s, hundreds of billions of devices are expected to be connected to the Internet. A vast amount of data and information will be constantly being formed, but if the data is siloed, it will be impossible to share it.

Therefore, it is necessary to create a wearable device that can constantly hold and share data. In order to achieve this, electronic devices with ubiquitous functions are expected to be realized as wearable devices, and flexible shapes, light weight, large area, and optically transparent functions are expected to be necessary.

Conductive oxide thin films such as indium-tin-oxide (ITO) and zinc oxide (ZnO) are expected to be the key semiconductor elements for wearable devices, but the manufacturing method to obtain conductive thin films with high electrical properties has not been established. ZnO thin films, which are introduced in this chapter, show great promise as photomechanical materials for photography [1, 2] and electrochemical and biosensor materials for various devices [3–7], and the applications of these thin films are diverse, including transparent electrodes, solar cells, and memory storage devices. When metal oxide thin films are used as optical films for liquid crystal displays and touch panels, both high transparency and low resistivity are required. At present, the aforementioned indium-tin oxide (ITO) and tin oxide are used in combination with other transparent materials. However, due to the low reserves of indium, it is expected to be depleted as a resource, and there is a need to search for alternative conductive materials, and research and development of alternative material technology has been conducted for many years. Research on ZnO has a history as long as that of ITO, and has produced many interesting results in recent years. ZnO has been grown by a number of methods, including sputtering [8–12], chemical vapor deposition [13], pulsed laser deposition [14], and wet coating [15]. Each of these methods for growing ZnO introduces high conductance and high transparency properties into the film but high-performance ZnO films have yet to be fabricated using low-cost, simple processes. The low-cost process is characterized by a fast growth rate at low temperatures. However, ZnO fabrication techniques are sensitive to growth temperature, atmospheric pressure, and oxygen concentration, making it difficult to synthesize uniform ZnO films. In addition, the high dependence on the performance of the synthesis equipment has made it impossible to achieve a uniform crystal structure at low temperatures as well as a high growth rate. Therefore, we aimed to establish a simple, low-cost and stable fabrication process based on the wet coating method for growing ZnO films.

In this chapter, the author explains the need for a technological breakthrough to form oxide conductive thin films with stable conductivity on plastic films in order to utilize ZnO thin films as highly functional films for processing large amounts of data while maintaining their flexibility. The conductivity mechanism of oxide conductive materials has been inferred from indirect data such as the dependence of conductivity on oxygen partial pressure [1, 2]. In particular, ZnO, along with ITO, was first discovered as a semiconductor in the 1930s. Since then, its optical transparency in the visible range has been exploited, and research and development on its optical and electrical properties have been conducted for use as a transparent conductive film in memory devices, photovoltaics, transistors, and other applications. Furthermore, ZnO has a high carrier electron concentration, which is due to the potential presence of crystal defects caused by dopants and contaminants intervening in the crystal during ZnO synthesis. The problem of the electron mobility limit of ZnO has been clarified to some extent by a great deal of research and development into methods of ZnO synthesis and optimal selection of dopants. Although some progress has been made with ZnO thin films, they still do not have the high-performance characteristics to withstand the mega-data processing that will be required in IoT devices. The decrease in mobility is attributed to grain boundary scattering and ionized impurity scattering depending on the grain size, and the control mechanism of electrical properties differs depending on the synthesis form, such as thin film or nanowire.

Therefore, the author focused on the “non-equilibrium reaction field” as a bottom-up architecture. Although many studies have been reported on the control of one-dimensional nanowire growth and the physical properties of the composites by moving the atomic and molecular groups constituting the oxide particles without heating, no technology has been found to create thin-film nanocomposite structures in a simple two-dimensional process. In this study, the author succeeded in discovering the basis of this technology by using an electron source that emits electrons uniformly in a plane. In addition, we will elucidate the interfacial phenomena and crosslinking mechanisms that occur during the bonding of metal oxide particles, and clarify the effects on the physical properties of the interface, mechanical properties, optical properties, and electronic structure. In addition, the author aims to create low-dimensional nanomaterials based on heterogeneous oxide-metal bonding with various dimensions, construct hybrid structures, control nanostructures, surfaces and interfaces, and control higher-order functional properties in metal-ceramics-semiconductor composites, and provide next-generation nanodevice components in a broad sense.

2. Experiment

2.1 Nanoscale ZnO particle synthesis

Zinc nitrate ($\text{Zn}(\text{NO}_3)_2$) (high purity chemistry), ammonium carbonate ($(\text{NH}_4)_2\text{CO}_3$) (high purity chemistry), ethanol, and deionized water are used. Deionized water is purified to high purity water using a distillation vessel, and 1.0 M zinc nitrate and ammonium carbonate are dissolved in high purity water respectively. The zinc nitrate solution is dropped into the strongly stirred ammonium carbonate solution and reacts in a molar ratio of 1:1.5 (= $\text{Zn}(\text{NO}_3)_2$: $(\text{NH}_4)_2\text{CO}_3$) to synthesize a white precipitate. The precipitate was filtered and cleaned several times with high-purity water and ethanol, and then dried at 100 °C in air for 6 hours to form the precursor of zinc oxide. The ZnO particles were then sintered at 400 °C for 4 hours in an electric furnace to obtain ZnO particles [16–18]. The obtained ZnO particles had a median diameter of 0.18 $\mu\text{m}\phi$, with 89% of the synthesized particles distributed between 0.12 and 0.25 $\mu\text{m}\phi$. The powder is represented in **Figure 1**.

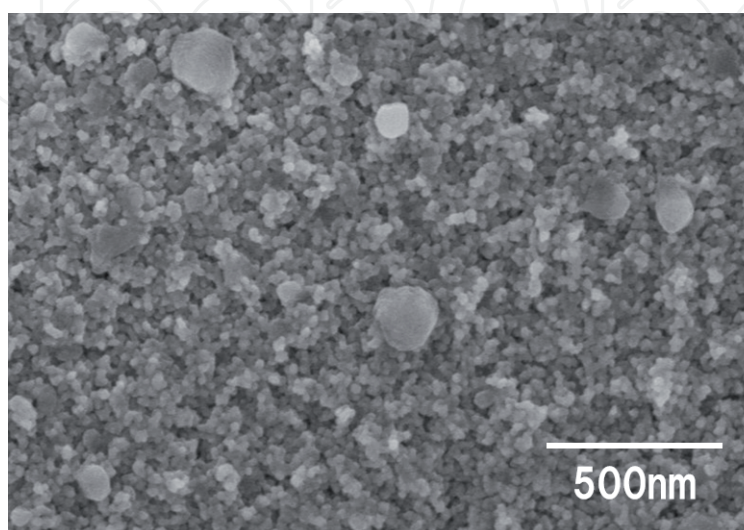


Figure 1.
ZnO nanoparticles.

2.2 Thin film formation

Prepare a coating of ZnO particles with zinc complex (zinc acetylacetonate (Zn(AcAc)), propanol (2-propanol) and a small amount of surfactant (thiol). See **Table 1** for the weight ratio; the ZnO particles were agglomerated and thiol was used to disperse them. The ZnO particles were agglomerated and thiol was used to disperse them. For the mixed solution of ZnO particles and Zn(AcAc) prepared in this study, the location of Zn(AcAc) in the residual solution after filtration of ZnO particles was not confirmed by Fourier Transform Infrared Spectroscopy (FT-IR). Zn(AcAc) was adsorbed on the zinc oxide surface. It is expected that Zn(AcAc) is electrostatically adsorbed on the surface of particles in the paint and the complexes serve as seeds for cross-linking between ZnO particles and promote the formation of ZnO thin films in two dimensions [19]. No solvent is added to act as a binder, and the coating is used to form a thin film. Plastic films with high transmittance, such as polyethylene terephthalate (PET) or polycarbonate film (PC), can be used as substrates to support the thin film. For thin film formation, a spray method was used, and a thin film with a thickness of 80 μm was applied before drying. The thin film was then dried using dry air at 60 $^{\circ}\text{C}$ to volatilize the solvent (propanol) and form a foil with only solids. At this point, the foil formed on the substrate is an aggregate of fine particles and almost no adhesion has occurred.

2.3 Field emission electron beam from hc-SWCNTs as a non-equilibrium excitation reaction field

In order to realize uniform planar electron emission as a non-equilibrium reaction field, it is essential to employ highly crystalline single-walled carbon nanotubes (hc-SWCNTs) in electrical devices as field emitters, and the effect of increasing the crystallinity of SWCNTs on electrical properties has been investigated [20, 21]. We employed hc-SWCNTs as field emission (FE) electron sources with a weight density of less than 1.3 mg/cm^2 and fabricated electrodes on graphite plates by electrostatic coating method. The FE electron source as the cathode electrode to induce FE was then grooved by physically carving the coating film to expose the hc-SWCNTs as the field emitter [20]. The electron source was stacked with an FE cathode fabricated with hc-SWCNTs to emit electrons, a gate electrode to block the FE electrons, an accelerator to adjust the acceleration energy of the FE beam from 0 to 120 kV, and an anode electrode placed on the ZnO particles, as shown in **Figure 2a**. Ever since Rinzler et al. predicted the possibility of electronic devices using CNTs in their landmark paper [22], carbon nanostructures with one-dimensional shapes have attracted much attention for their applications in electronic and electrical devices. The hc-SWCNTs have excellent physicochemical properties. Tohji et al. succeeded in synthesizing pure hc-SWCNTs by purification and annealing at high temperature of 1473 K and low pressure of less than 10^{-5} Pa [23]. We also established a method to evaluate the crystallinity of SWCNTs by using cryogenic thermal desorption spectroscopy and high-resolution transmission electron microscopy (HR-TEM, Hitachi High-Technologies) [24]. The HR-TEM image of such a crystal is shown in **Figure 2b**. We succeeded in uniformly dispersing hc-SWCNTs [23], which have

	ZnO	Thiol	Zinc acetylacetonate	Solvent
Composition ratio of mixture (wt%)	16.9	4.3	6.8	72.0

Table 1.
ZnO thin film formation condition in this study.

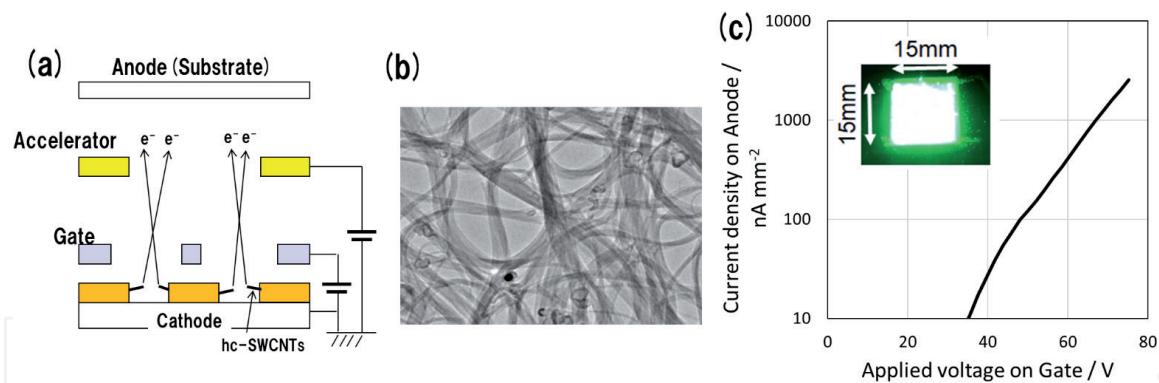


Figure 2. FE source using hc-SWCNTs. (a) Structure of FE source with high energy electron beam to fabricate ceramic nanostructure. (b) HR-TEM image of hc-SWCNTs after crystallization. (c) FE characteristics between cathode and anode electrodes and image of lighting emitted by a planar FE cathode (inset).

excellent physicochemical properties, and they have been employed as field emitters to produce uniform planar FE electron emission over a wide range of electron emission currents, as shown in **Figure 2c**. It is difficult to form ZnO particles with uniform morphology and crystal structure when the variation of the dose in the plane is more than 0.5%. Controlling the intensity of the electron beam in the plane is essential for fabricating devices that can serve as electron sources.

It is speculated that the nanoscale Zn grains rotate and vibrate when irradiated with electrons of up to 120 keV using the system shown in **Figure 2a** [25], and that each Zn terminal interface after electron irradiation is activated as a non-equilibrium reaction field of appropriate energy of about 120 keV to bridge to other Zn atoms.

The possibility of using plastic films as substrates for general-purpose construction of key semiconductor elements for IoT devices may be well considered in the future. In order to investigate the process of device construction without heating considering the heat resistance of plastic, this study aims to form a two-dimensional continuous thin film by applying a non-equilibrium reaction field and using high-energy electron beam irradiation as the non-equilibrium reaction field.

2.4 Non-thermal formation of ZnO film on plastic film substrate by FE electron beam irradiation

We have developed a technique to fabricate ZnO thin films on thin PET substrates using FE electron beam irradiation as a non-equilibrium reaction field as shown in **Figure 3a**. The ZnO thin films were prepared by wet coating and electron beam irradiation methods [26, 27]. In this process, the thickness of the ZnO film was controlled from 100 nm to 10 μm . The FE current density emitted from each hc-SWCNT as an electron emission source was controlled to about 20 pA/cm^2 , which corresponds to 10^{13} electrons/ cm^2 -s for the preparation of the films. The electrical and optical properties of carrier density, hole mobility, resistivity and optical transmittance at 550 nm wavelength were evaluated for ZnO thin films of about 100 nm thickness fabricated by using 120 keV FE electron beam as basic properties. 120 keV FE electron beam irradiated ZnO thin films showed carrier density The ZnO thin films prepared by irradiation of 120 keV FE electron beam showed carrier density of $1.8 \times 10^{18} \text{ cm}^{-3}$, hole mobility of $158.6 \text{ cm}^2/\text{Vs}$, resistivity of $8.6 \times 10^{-4} \Omega\text{-cm}$ and optical transmittance of 78% at 550 nm wavelength. Although attempts to improve the electrical properties of ZnO thin films using various synthetic techniques have been reported, the fabrication of highly functional

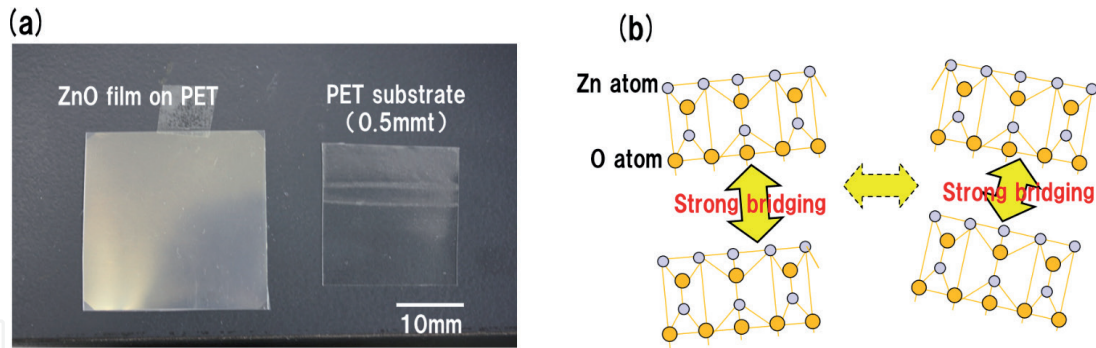


Figure 3. (a) Images of (left) ZnO thin film synthesized on a PET substrate with irradiation of electron energy of 120 keV and (right) a bare PET substrate. (b) Schematic diagram showing bridging of ZnO crystal.

ZnO thin films on plastic films at low temperatures has not yet been done due to the temperature limitations of the substrate supporting the films. Considering the defects that stabilize the sites between the anti-sites, it is important to (1) clarify the interfacial phenomena and bridging mechanisms that selectively occur in the c-axis direction during the bonding of the terminal crystal interface of metal oxide particles as shown in **Figure 3b**, and (2) determine how to fabricate stable ZnO thin films on plastic substrates due to the constraints related to the temperature of the substrate supporting the thin films, (2) electron irradiation and acceleration energy of electron beam are necessary for crystal structure rearrangement and film synthesis after ZnO grain formation. In the present work, we propose to form ZnO bulk by FE electron beam irradiation during bridging between ZnO grains and to fabricate ceramic thin films without heat treatment.

By using non-equilibrium reaction fields as a bottom-up tool for the formation of oxide thin films, we have discovered a process technology for the formation of ZnO thin films on PET film substrates. The thin films obtained by this process have been evaluated for their conductive properties. In this study, we have evaluated the basic physical properties of this thin film such as carrier density, hole mobility, resistivity and optical transmittance. The results are shown in **Figure 4** for carrier density, hole mobility and resistivity, and **Figure 5** for transmittance [26]. We have succeeded in finding that each property differs depending on the electron beam irradiation energy. ZnO thin films grown at electron energy of 120 keV have electrical properties of carrier density of $1.8 \times 10^{18} \text{ cm}^{-3}$ and hole mobility of $208.6 \text{ cm}^2/\text{Vs}$, and resistivity of $8.6 \times 10^{-4} \Omega\text{-cm}$. However, due to the limitations of the ZnO (plus dopant) formation temperature and the substrate on which the thin film is supported, low-temperature ZnO formation has not yet yielded highly functional thin films in terms of hole mobility and resistivity. O atoms, and

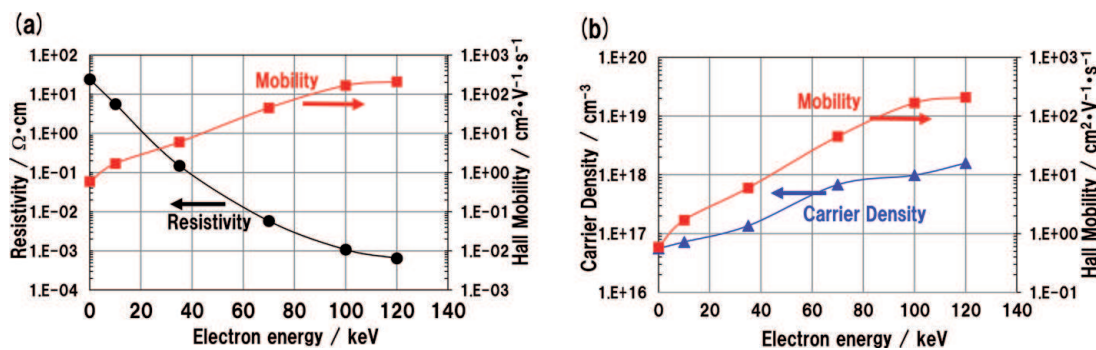


Figure 4. (a) Resistivity and hole mobility dependence on electron beam irradiation energy, (b) carrier density and hole mobility dependence on electron beam irradiation energy.

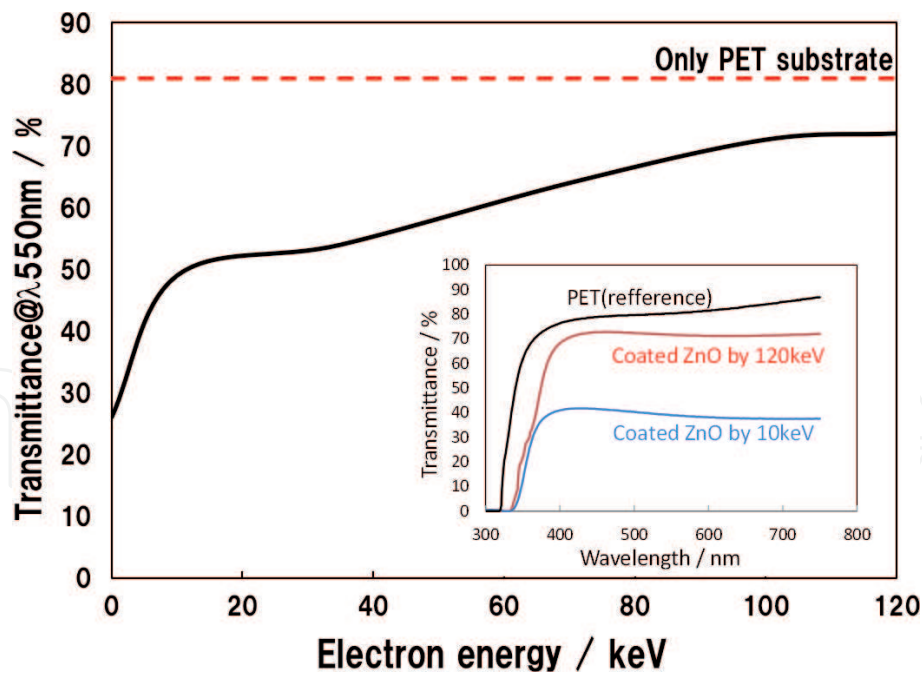


Figure 5. Spectral transmittance of ZnO thin film on PET substrate as a function of electron irradiation energy at 550 nm. The red dotted line in the graph shows the transmittance at 550 nm for PET substrate only, and the inset shows the spectral transmittance for PET substrate only at electron irradiation energy of 10 keV (blue solid line) and 120 keV (red solid line).

complex defects that stabilize Zn interstitials and Zn anti-sites, the technology to build stable ZnO thin films or bulk structures has not been established. It has been reported that strict and stable control of the deposition environment is necessary from the time of ZnO formation with regard to oxygen defects and defects in the crystal concept, and that rearrangement of the crystal structure and control of crystal defects by annealing at 500 K or higher after the formation of the thin film are necessary to improve electrical properties [28, 29]. In our proposal, a thin film is formed by Zn cross-linking between ZnO particles and Zn partial oxidation by controlling the oxygen atmosphere during film formation without using a heating process, and we assume that the cross-linked Zn plays the role of atoms close to n-type dopants. As for the transmittance (**Figure 5**), it shows the dependence of transmittance on electron beam irradiation energy at 550 nm. The ZnO thin film has a band gap of about 3.7 eV and was found to have a crystalline structure similar to the bulk structure [29, 30].

The transmittance of the ZnO thin film was 70% @ λ 550nm, the same as that of the PET substrate, and **Figure 5** shows that there is still room for improvement in the transmittance.

3. Discussion

3.1 Crystallization process of ZnO particles

The surface morphology and composition distribution of ZnO particles on PET film substrates were observed by Scanning Electron Microscope (SEM; Hitachi High-Technologies Co., Ltd., Japan) and Electron Probe Micro Analyzer (EPMA; JEOL). **Figure 6a** shows the surface morphology of the coating during the formation of ZnO thin film, and **Figure 6b** and **c** show the surface morphology of the coating after plasma treatment. **Figure 6b–e** show the compositional separation of ZnO particles as oxide and Zn (including Zn ions) as metal, analyzed by EPMA.

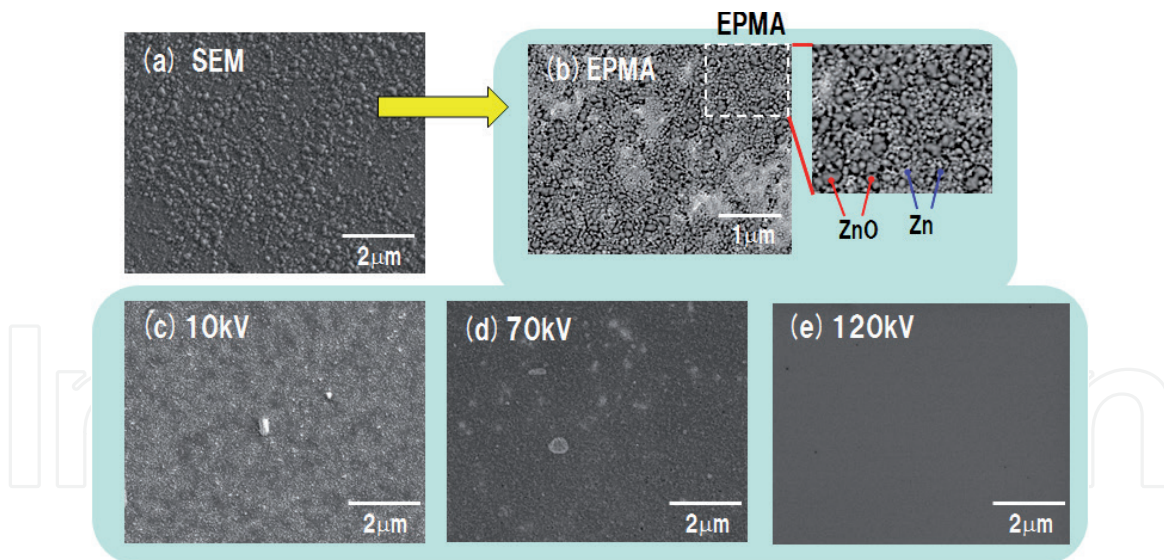


Figure 6.

The surface after ZnO coating (a) SEM after plasma treatment, (b) EPMA of the film surface after plasma treatment, (c) EPMA of the film surface after 10 keV electron beam irradiation, (d) EPMA of the film surface after 70 keV electron beam irradiation, (e) EPMA of the film surface after 120 keV electron beam irradiation.

Figure 6b shows the uniform dispersion of ZnO particles and Zn ions in submicron order and the close relationship between ZnO particles (gray) and Zn ions (white) in the coating film after plasma treatment. Ions (white) can be confirmed. Furthermore, **Figure 6c–e** show the EPMA images of the surface after irradiation with 10, 70 and 120 KeV electron beams. As the electron beam energy intensity increased, the distribution of Zn ions, represented by white color, disappeared and was found to be dominated by ZnO. However, it is difficult to form ZnO thin films with uniform composition and crystal structure when the in-plane dose density variation is more than 0.5%, and the control of the in-plane electron dose is a very important performance in the construction of electron source devices.

The electron diffraction patterns of (a) and (e) are shown in **Figure 7** using a Transmission Electron Microscope (TEM; JEOL). For the thin film immediately after coating, it represents a mass of submicron sized ZnO particles, i.e., polycrystalline structure, and it can be seen that there are individual particles with aligned crystallinity in random directions. In the crosslinking between ZnO particles, diffraction grating images along the C axis were observed, and the internal crystalline structure of the particles themselves was retained in the direction along the a and b axes. In the crosslinking between ZnO particles, diffraction grating images along the C-axis were observed, suggesting that a crystal structure similar to that of ZnO was constructed between the particles in the direction along the a- and b-axes while the internal crystal structure of the particles was retained.

The macrocrystalline structure of ZnO thin film formed by electron beam irradiation was analyzed by X-Ray diffraction (XRD; Rigaku) for its dependence on electron beam irradiation energy (**Figure 8** [26]). It was found that the grain size of ZnO-derived single crystals increased with increasing electron beam energy, indicating that the electron beam irradiation energy promoted grain cross-linking, i.e., crystal growth. Adsorbed on the ZnO particles were observed to cross-link with ZnO while aligning the crystal direction by plasma exposure and electron beam irradiation.

We were able to obtain different electrical properties depending on the process conditions of the non-equilibrium reaction field without changing the materials that make up the ZnO film. The change in the electrical properties of ZnO, especially the mobility (carrier density), is mostly due to the scattering of electrons and holes in the ZnO crystal structure by ionized impurities or grain boundaries.

The degree of scattering is greatly influenced by the control of crystallinity. In this study, only ZnO particles and zinc complexes were used for ZnO thin film formation, and we tried to analyze the surface state of ZnO to investigate factors other than the effect of dopants.

Figure 9 shows the results of X-ray Photoelectron Spectroscopy (XPS; Bruker) analysis of ZnO particles only. The binding energy of Zn intercalated in the

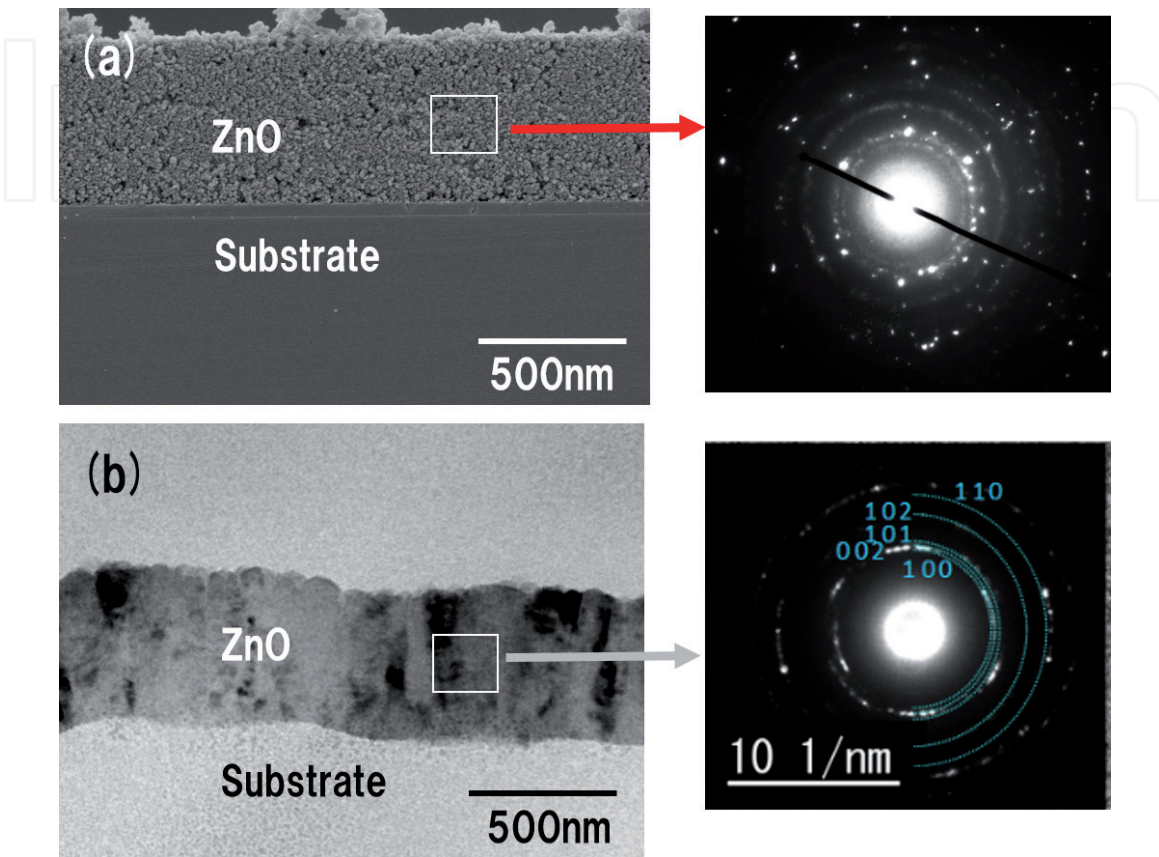


Figure 7.
(a) SEM observation and TEM diffraction image of the film cross-section after coating process, (b) TEM observation and diffraction image of the film cross-section after 120 keV electron beam irradiation.

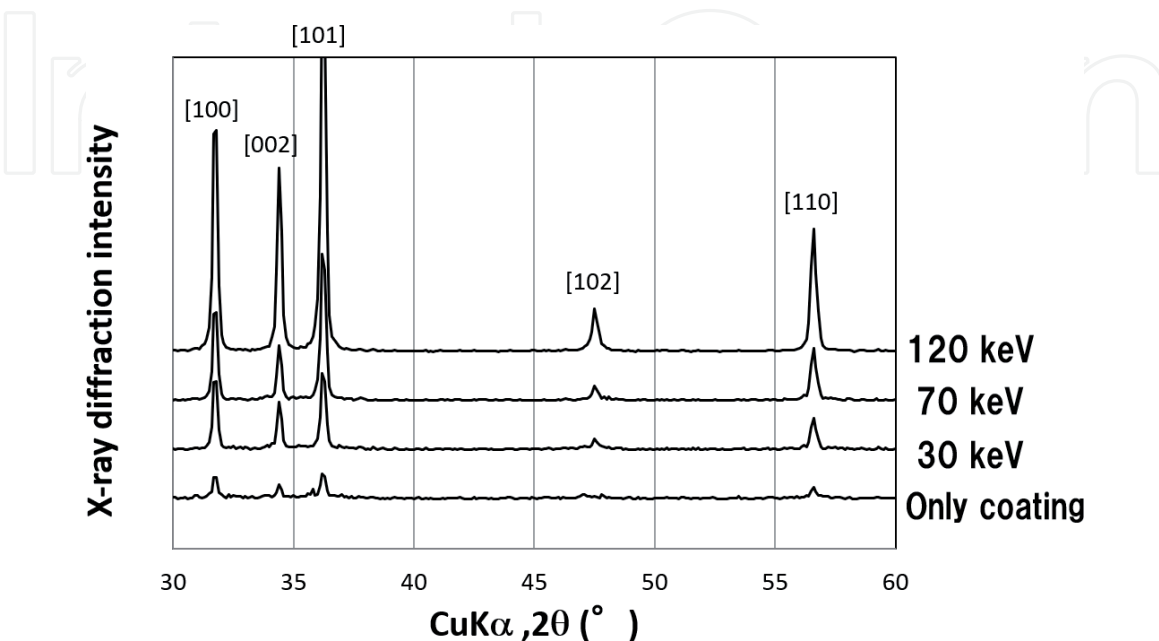


Figure 8.
XRD patterns of ZnO thin films after plasma treatment and electron irradiation.

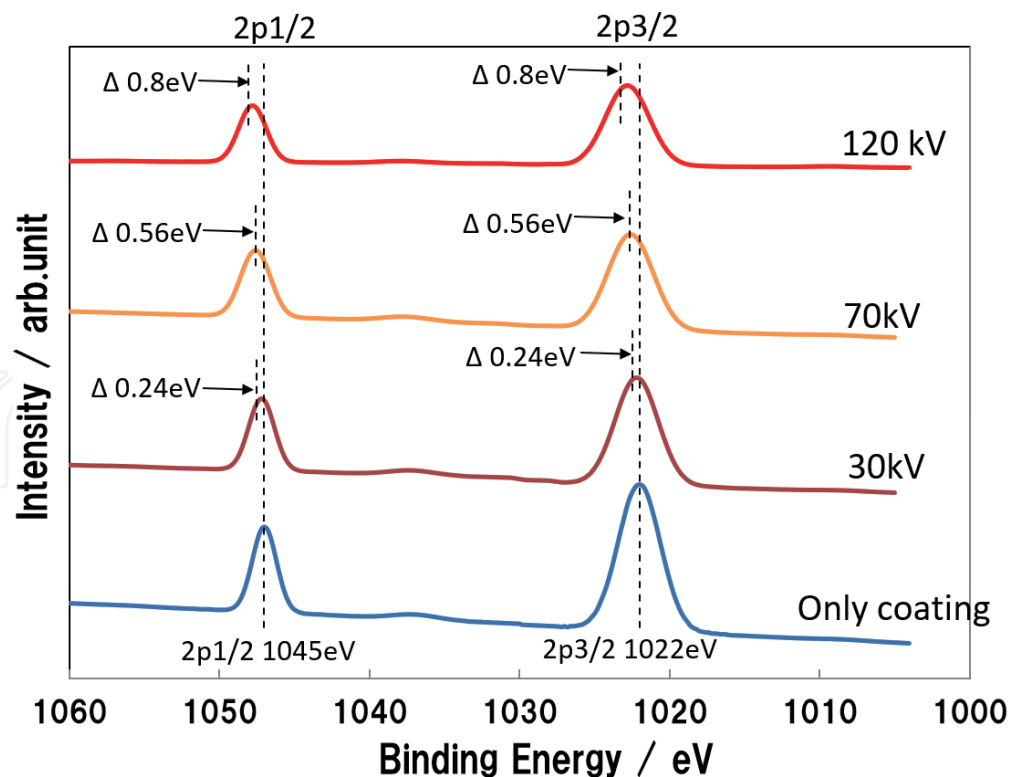


Figure 9. Binding energy transitions of Zn $2p_{3/2}$ and $2p_{1/2}$ after plasma treatment and electron beam energy of 30, 70 and 120 keV irradiation of ZnO thin films by XPS.

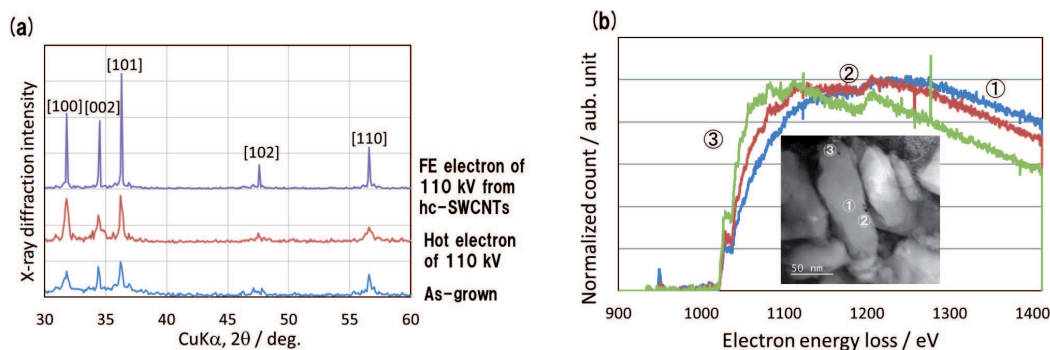


Figure 10. Zinc spectrum of a ZnO particle synthesized by electron beam irradiation. The inset shows the measured points on the particle.

particle surface was evaluated [26]. The ZnO particles with Zn ions adsorbed from Zn(AcAc) from plasma treatment were irradiated with electron beam and it was found that the binding energy of Zn $2p_{3/2}$ and Zn $2p_{1/2}$ shifted to higher energy side with the increase of electron beam energy. In particular, when the electron beam energy is 110 keV, the binding energy is increased by 0.8 eV. Due to the increase in binding energy, the valence electron density of states decreases, i.e., the oxidation number increases. It is speculated that electron beam irradiation makes Zn and ZnO particle surfaces more susceptible to oxidation, and that defects such as oxygen defects and interstitial zinc on ZnO surfaces are oxidized and bound.

Figure 10 shows the spectra of zinc in ZnO particles synthesized by 120 keV electron beam irradiation, obtained from electron energy loss spectroscopy (EELS; Gatan Corporation) [31]. The measurement points were the edges of the short and long axes and the center of the ellipsoidal particles, as shown in **Figure 10b**. The spectra obtained at both edges of the particle (point 2 and point 3 in the inset of **Figure 10b**)

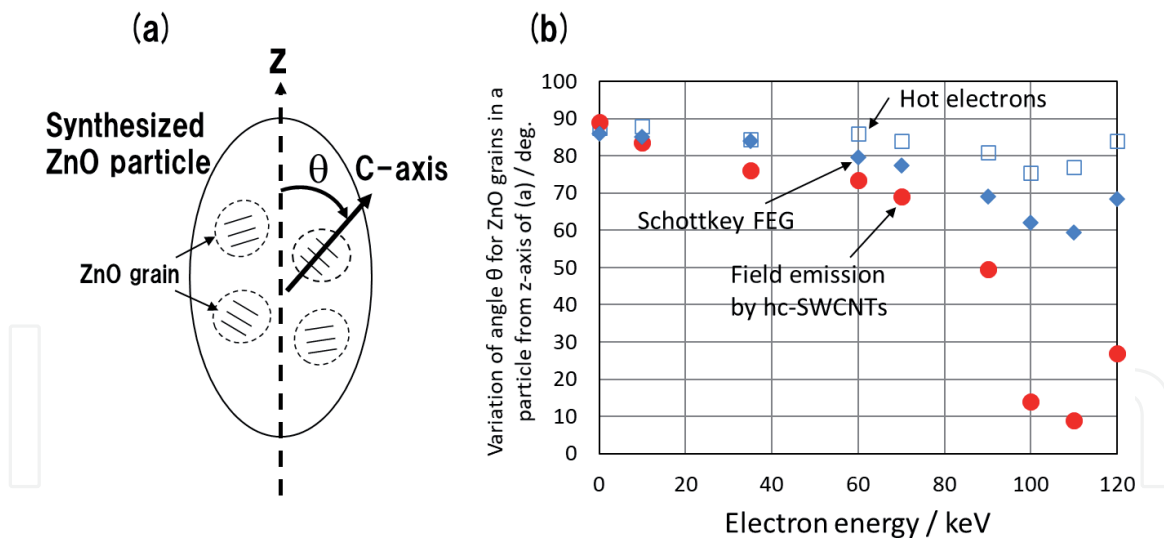


Figure 11. Dependence of the c-axis direction and the angle from the major axis of the ZnO particles observed after electron irradiation at acceleration voltages from 0 to 120 keV. (a) Schematic diagram showing the angle between the long axis of the synthesized particles and the c-axis direction of each ZnO particle in the particles. (b) Schematic diagram showing the dependence of the angle change from the c-axis direction on the electron energy of the electron beam.

were different from those obtained at point 1 in the inset of **Figure 10b**. The spectrum obtained at point 1 provided information about the ZnO bulk. The zinc terminal interfaces of the ZnO particles synthesized by electron irradiation had different compositions and complex electrical states, and the interface belonging to the long axis of the particles (c-axis of ZnO) was found to activate the crystal bridging [32–35].

3.2 Analysis of crystal orientation of synthesized ZnO particles

The angle between the long axis, meaning the direction of the elongated ZnO particles aggregated with nanoscale ZnO particles in the synthesized particles, and the c-axis of each ZnO particle in the synthesized particles is shown in **Figure 11a**, and the angular distribution along the long axis of the particles as shown in **Figure 11b** was obtained by TEM [31]. **Figure 11b** shows the variation dependence of the angle obtained by clockwise rotation between the c-axis of each ZnO particle in the ZnO composite particles and the z-axis in **Figure 11a** on the electron energy of each electron source. The range of the angle is from 0 to 90 degrees. The results show that the c-axis of each ZnO grain in the particle is aligned with high energy resolution and high acceleration energy of about 90–120 keV. In particular, the crystallization of ZnO particles by FE electron beam irradiation resulted in fine bridges between the c-axes of each formed grain. For the electron-beam treated ZnO particles, aggregation of nanoscale ZnO particles, i.e., polycrystalline structure, was observed with crystallographically continuous structure along the c-axis similar to that of bulk ZnO crystals, indicating the distribution of individual nanoscale grains with an ordered crystal structure. The energy resolution of the electron beam depends on the electron emission mechanism.

4. Conclusion

We have developed a method for non-thermal cross-linking of ZnO particles by FE electron beam irradiation as a non-equilibrium reaction field. In order to enhance the crystallinity of ceramic materials, it is necessary to control the energy

resolution and acceleration of the electron beam. In this study, an FE electron beam source with a low energy resolution and a half-value width of less than 100 meV was employed. By irradiating FE electron beams with a dose of less than 0.5% in the plane, the energy of the terminal crystalline interface of ZnO nanoscale particles was activated and the zinc ions decomposed from the ZnO particles where bridging was achieved. Thus, by energy exchange between each ZnO particle, the zinc was connected to the zinc or oxide of other site atoms. Furthermore, the processing architecture obtained in this study allowed us to fabricate ZnO thin films with good electrical properties on PET film substrates. In the future, we will aim to obtain higher electrical and optical properties by synthesizing ZnO thin films on PET film by controlling the adhesion between ZnO and substrate and the crystal orientation of the ZnO layer near the substrate. If we can control the crystal orientation and nanostructure of the ceramic film near the substrate, we expect to be able to fabricate ceramic thin films (layers) on top of other materials, semiconductors, or other ceramic layers.

This bottom-up architecture will also enable us to (1) determine the interfacial properties and their effect on the electronic structure, and (2) control the nanostructured end-crystalline interface to provide the basic elements for a wide range of next-generation devices by using composites of metals, ceramics, and semiconductors to achieve highly functional properties.

IntechOpen

Author details

Norihiro Shimoi

Department of Electrical and Electronic Engineering, Tohoku Institute of Technology, Sendai, Japan

*Address all correspondence to: n-shimoi@tohotech.ac.jp

IntechOpen

© 2021 The Author(s). Licensee IntechOpen. This chapter is distributed under the terms of the Creative Commons Attribution License (<http://creativecommons.org/licenses/by/3.0>), which permits unrestricted use, distribution, and reproduction in any medium, provided the original work is properly cited. 

References

- [1] T. Minami, "Transparent and conductive multicomponent oxide films prepared by magnetron sputtering." *J. Vac. Sci. Technol. A* 17, 1765 (1999).
- [2] J. Suskia, D. Largeau, A. Steyer, V. D. Polb and F.R. Blomb, "Optically activated ZnO/SiO₂/Si cantilever beams." *Sens. Actuat. A: Physical*, 24, 3, 221-225 (1990).
- [3] S. Masuda, K. Kitamura, Y. Okumura, S. Miyatake, H. Tabata and T. Kawai, "Transparent thin film transistors using ZnO as an active channel layer and their electrical properties." *J. Appl. Phys.* 93, 1624 (2003).
- [4] Y. Furubayashi, T. Hitosugi, Y. Yamamoto, K. Inada, G. Kinoda, Y. Hirose, T. Shimada, and T. Hasegawa, "A transparent metal: Nb-doped anatase TiO₂." *Appl. Phys. Lett.* 86, 252101 (2005).
- [5] C.-Y. Lee, Y.-T. Haung, W.-F. Su, and C.-F. Lin, "Electroluminescence from ZnO nanoparticles/organic nanocomposites." *Appl. Phys. Lett.* 89, 231116 (2006).
- [6] H. Kawazoe, M. Yasukawa, H. Hyodo, M. Kurita, H. Yanagi, and H. Hosono, "P-type electrical conduction in transparent thin films of CuAlO₂." *Nature*, 389, 939 (1997).
- [7] P.-H. Yeh, Z. Li, and Z. L. Wang, "Schottky-Gated Probe-Free ZnO Nanowire Biosensor." *Adv. Mater.* 21, 4975 (2009).
- [8] I.A. Rauf, "A novel method for preparing thin films with selective doping in a single evaporation step." *J. Mater. Sci. Lett.*, 12, 1902 (1993).
- [9] H. Ohta, M. Orita, M. Hirano, H. Tanji, H. Kawazoe and H. Hosono, "Highly electrically conductive indium-tin-oxide thin films epitaxially grown on yttria-stabilized zirconia (100) by pulsed-laser deposition." *Appl. Phys. Lett.* 76, 2740 (2000).
- [10] T. Minami, T. Miyata, Y. Ohtani, and Y. Mochizuki, "New Transparent Conducting Al-doped ZnO Film Preparation Techniques for Improving Resistivity Distribution in Magnetron Sputtering Deposition." *Jpn. J. Appl. Phys.* 45, L409 (2006).
- [11] M. Kon, P. K. Song, Y. Shigesato, P. Frachl, A. Mizukami, and K. Suzuki, "Al-Doped ZnO Films Deposited by Reactive Magnetron Sputtering in Mid-Frequency Mode with Dual Cathodes." *Jpn. J. Appl. Phys.* 41, 814 (2002).
- [12] N. Malkomes, M. Vergohl and B. Szyszka, "Properties of aluminum-doped zinc oxide films deposited by high rate mid-frequency reactive magnetron sputtering." *J. Vac. Sci. Technol. A* 19, 414 (2001).
- [13] S. Ohnishi, Y. Hirokawa, T. Shiosaki, and A. Kawabata, "Chemical Vapor Deposition of Single-Crystalline ZnO Film with Smooth Surface on Intermediately Sputtered ZnO Thin Film on Sapphire." *Jpn. J. Appl. Phys.* 17, 773 (1978).
- [14] R. D. Vispute, V. Talyansky, Z. Trajanovic, S. Choopun, M. Downes, R. P. Sharma, T. Venkatesan, M. C. Woods, R. T. Lareau, K. A. Jones and A. A. Iliadis, "High quality crystalline ZnO buffer layers on sapphire (001) by pulsed laser deposition for III-V nitrides." *Appl. Phys. Lett.* 70, 2735 (1997).
- [15] S. major, A. Banerjee, and K. L. Chopra, "Highly transparent and conducting indium-doped zinc oxide films by spray pyrolysis." *Thin Solid Films*, 108, 333 (1983).

- [16] O. Mahian, A. Kianifar, and S. Wongwises, "Dispersion of ZnO Nanoparticles in a Mixture of Ethylene Glycol–Water, Exploration of Temperature-Dependent Density, and Sensitivity Analysis." *J. Clust. Sci.* 24, 1103-1114 (2013).
- [17] N. Uekawa, J. Kajiwara, N. Mochizuki, K. Kakegawa, and Y. Sasaki, "Synthesis of ZnO nanoparticles by decomposition of zinc peroxide." *Chem. Lett.* 30, 606-607 (2001).
- [18] N. Uekawa, N. Mochizuki, J. Kajiwara, F. Mori, Y. J. Wu, and K. Kakegawa, "Nonstoichiometric properties of zinc oxide nanoparticles prepared by decomposition of zinc peroxide." *Phys. Chem. Chem. Phys.* 5, 929-934 (2003).
- [19] N. Shimoi, T. Harada, Y. Tanaka, and S.-I. Tanaka, "Controlling the electrical properties of ZnO films by forming zinc and oxide bridges by a plasma and electron-assisted process." *AIP Adv.* 2, 22167 (2012).
- [20] N. Shimoi, L. E. Adriana, Y. Tanaka, K. Tohji, "Properties of a field emission lighting plane employing highly crystalline single-walled carbon nanotubes fabricated by simple processes," *Carbon* 65, 228-235 (2013).
- [21] N. Shimoi, Y. Sato, K. Tohji, "Highly Crystalline Single-walled Carbon Nanotube Field Emitters: Energy-loss-free High Current Output and Long Durability with High Power," *ACS Appl. Electron. Mater.* 1, 163-171 (2019).
- [22] A. G. Rinzler, J. H. Hafner, P. Nikolaev, L. Lou, S. G. Kim, D. Tománek, P. Nordlander, D. T. Colbert, R. E. Smalley, "Unraveling Nanotubes: Field Emission from an Atomic Wire," *Science* 269, 1550-1553 (1995).
- [23] K. Tohji, T. Goto, H. Takahashi, Y. Shinoda, N. Shimizu, B. Jeyadevan, I. Matsuoka, Y. Saito, A. Kasuya, T. Ohsuna, K. Hiraga, Y. Nishina, "Purifying single-walled nanotubes," *Nature* 383, 679 (1996).
- [24] S. Iwata, Y. Sato, K. Nakai, S. Ogura, T. Okano, M. Namura, A. Kasuya, K. Tohji, K. Fukutani, "Novel method to evaluate the carbon network of single-walled carbon nanotubes by hydrogen physisorption," *J. Phys. Chem. C* 111, 14937-14941 (2007).
- [25] B.-S. Xu, S.-I. Tanaka, "Behavior and bonding mechanisms of aluminum nanoparticles by electron beam irradiation," *NanoStructured Materials* 12, 915-918 (1999).
- [26] N. Shimoi, S.-I. Tanaka, "Nonthermal crystal bridging of ZnO nanoparticles by nonequilibrium excitation reaction of electrons and plasma without cross-linking agent on plastic substrate," *J. Alloys and Comp.* 797, 676-683 (2019).
- [27] N. Shimoi, T. Harada, Y. Tanaka, S.-I. Tanaka, "Controlling the electrical properties of ZnO films by forming zinc and oxide bridges by a plasma and electron-assisted process," *AIP Advances* 2, 022167 (2012).
- [28] D. C. Look, J. W. Hemsky, and J. R. Sizelove, "Residual Native Shallow Donor in ZnO." *Phys. Rev. Lett.* 82 (1999) 2552-2555.
- [29] K. Ellmer, "Resistivity of polycrystalline zinc oxide films: current status and physical limit." *J. Phys. D: Appl. Phys.* 34 (2001) 3097-3108.
- [30] M. Xia, Z. Cheng, J. Han, M. Zheng, C.-H. Sow, J. T. L. Thong, S. Zhang, and B. Li, "Gallium ion implantation greatly reduces thermal conductivity and enhances electronic one of ZnO nanowires." *AIP Adv.* 4 (2014) 57128.
- [31] N. Shimoi, and S.-I. Tanaka, "Nonthermal and selective crystal bridging of ZnO grains by irradiation

with electron beam as nonequilibrium reaction field,” *Rev. Sci. Instrum.* 92, 023905 (2021).

[32] W. P. Vellinga, J. TH. M. De Hosson, “Atomic structure and orientation relations of interfaces between Ag and ZnO,” *Acta Mater.* 45, 933-950 (1997).

[33] K. Murakami, M. Saito, E. Takuma, H. Ichinose, “ARHVTEM of Pd/ZnO heterointerface chemical structure,” *J. Elec. Micro.* 52, 27-32 (2003).

[34] B. Meyer, D. Marx, “Density-functional study of Cu atoms, monolayers, films, and coadsorbates on polar ZnO surfaces,” *Phys. Rev. B* 69, 235420 (2004).

[35] S. B. Sinnott, E. C. Dickey, “Ceramic/metal interface structures and their relationship to atomic- and meso-scale properties,” *Mat. Sci. Eng. R* 43, 1-59 (2003).